JOURNAL OF CATALYSIS 73, 396–405 (1982)

Combined Temperature-Programmed Desorption and Infrared Study of H_2 Chemisorption on ZnO

G. L. GRIFFIN[1,2] AND J. T. YATES, JR.

Surface Science Division, National Bureau of Standards, Washington, D.C. 20234

Received June 23, 1981; revised November 2, 1981

The adsorption of H_2 on ZnO powders has been studied using the combined techniques of temperature-programmed desorption (TPD) and transmission infrared spectroscopy. The single previously observed ir-active state of dissociatively adsorbed H_2, which has stretching frequencies at $\nu_{Zn-H} = \sim 1710\ cm^{-1}$ and $\nu_{O-H} = \sim 3490\ cm^{-1}$, is found to desorb in two stages, characterized by maxima in the TPD spectra at ~240 and ~300 K. A new, low-temperature ir-active state has been observed with $\nu_{Zn-H} = \sim 1710\ cm^{-1}$ and $\nu_{O-H} = \sim 3455\ cm^{-1}$, which has a TPD maximum at ~170 K. Additional measurements of adsorption isotherms and adsorption rates indicate that the two states with TPD maxima at 240 and 300 K have comparable binding energies of 12.6 ± 1.0 kcal/mole, and are distinguished by different activation barriers for adsorption. The low-temperature adsorption state, which also exhibits an activation barrier for adsorption, has a binding energy of ~7 kcal/mole, and cannot be populated at room temperature.

INTRODUCTION

Zinc oxide is the primary component of commercial methanol synthesis catalysts (*1*). Its activity for olefin hydrogenation (*2*) and various photoassisted reactions (*3, 4*) has also been studied. In particular, Klier and co-workers (*5*) have suggested that the primary function of ZnO in methanol synthesis catalysts may be to provide sites for dissociative adsorption of H_2, as the initial step toward CO hydrogenation.

It is well known that at least one type of H_2 adsorption on ZnO involves dissociative adsorption onto Zn–O "pair" sites (*5–9*):

This has been labeled type I adsorption by Dent and Kokes (*10*), and is characterized by strong ir-absorbance maxima at 3490 and 1710 cm^{-1}, due to OH and ZnH stretching modes, respectively. However, a detailed description of the energetics of type I adsorption has not been reported. Such a description would be useful in determining the importance of this adsorption state as an intermediate in catalytic processes. In the existing temperature-programmed desorption (TPD) studies of H_2/ZnO, ir spectra of the adsorbed species were not recorded (*11, 12*), and thus the binding states indicated by the TPD spectra could not be unambiguously correlated with ir-active species.

In this paper we report on a combined ir and TPD study of type I H_2 adsorption on ZnO, using a sample cell which allows desorption rates and ir spectra of H_2 adsorbed on a single sample to be monitored. This allows features in the TPD spectra to be unambiguously related to the ir-active adsorption state.

EXPERIMENTAL

The sample cell is shown in Fig. 1. It is assembled from commercially available CaF_2 windows which sandwich a 2¾-in. flange into which the sample holder is mounted. The holder is a Cu ring, plated with Ni and Au layers to minimize the for-

[1] National Research Council Postdoctoral Research Associate, 1979–1980.

[2] Present address: Department of Chemical Engineering and Materials Science, University of Minnesota, Minneapolis, Minn. 55455.

0021-9517/82/020396-10$02.00/0

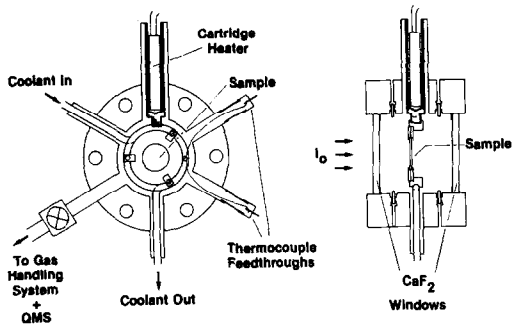

FIG. 1. UHV cell for simultaneous infrared and thermal temperature-programmed desorption spectroscopy.

mation of volatile CuO during sample preparation. A $\frac{1}{32}$-in. stainless-steel tube is soldered around the circumference of the ring in order to cool the sample using liquid N_2. A 50-W cartridge heater is inserted into the ring mount to heat the sample. An iron–constantan thermocouple is attached to the sample ring. The cell is connected to a stainless-steel, bakeable gas handling system for admitting and evacuating gases. Gas pressures are measured with capacitance manometers. Pumping is provided by a zeolite sorption pump and a 20 liter/s ion pump. A quadrupole mass spectrometer (Spectramass 1000 M) is used to monitor gas desorption rates during TPD experiments. A flexible connection between the gas handling system and the sample cell allows the cell to be positioned in the sample beam of the ir spectrometer (Perkin–Elmer-180).

A sample is prepared by pressing 0.25 g of ZnO (Kadox 25) at 25,000 psi in a die to form a $\frac{1}{2}$-in.-diameter disk. Once the sample is mounted, the cell is evacuated and then heated to 400°C for 3 h to activate the ZnO; H_2O and CO_2 are the main gases which evolve during the activation process. The sample is cooled under vacuum to 300°C, then to room temperature under 10 Torr of O_2, and finally the O_2 is pumped off. This O_2 treatment markedly improves the background transmission in the ir spectra (*7, 13*).

The standard procedure for TPD experiments was the following: The sample was brought to the desired temperature for H_2 exposure and the desired pressure of H_2 was admitted. If the exposure temperature was greater than 100 K, the sample was cooled to 100 K, and then the residual H_2 was evacuated. After all physisorbed H_2 was removed (*13*), the warm-up was begun. An approximately linear heating rate was obtained by steadily increasing the current through the cartridge heater. The H_2 desorption rate was monitored using the mass spectrometer. All of the TPD spectra were obtained with the ir beam blanked off from the sample, to eliminate the effect of additional warming by the ir beam.

RESULTS

The ir spectrum of H_2 reversibly adsorbed on ZnO is shown in Fig. 2. The upper spectrum was recorded with 70 Torr of H_2 in the cell, and the lower spectrum shows the sample after evacuation. Two stretching modes due to dissociatively adsorbed H_2 are observed: $\nu_{OH} = \sim 3490\ cm^{-1}$ and $\nu_{ZnH} = \sim 1710\ cm^{-1}$. These frequencies vary as a function of coverage, as discussed below. The remaining features in the spectra are due to residual OH (3600–3400 cm^{-1}) and carbonate-like structures (1700–1300 cm^{-1}) which remain after the thermal pretreatment (*14–16*).

The TPD spectra of H_2 desorbing from ZnO for various initial coverages are shown in Fig. 3. The coverages were varied by exposing the sample to different pressures of H_2 at room temperature, cooling the sample to 100 K, and pumping off the residual H_2. The following characteristics are noted:

(1) Three or possibly four temperature maxima are present. We shall label the peak near 170 K as desorption state I_a, the peak near 240 K as state I_b, and the broad region with peaks near 270 and 310 K as state I_c.

(2) There was residual gas to be pumped away at all but the lowest dosing pressure

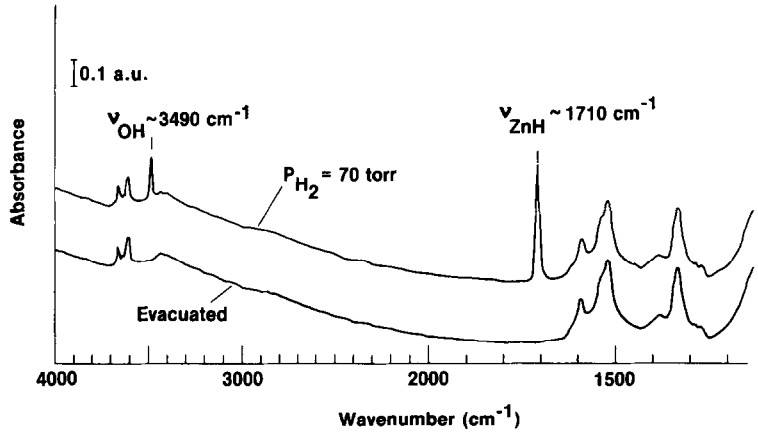

FIG. 2. Infrared spectrum of reversible (type I) H_2 adsorption on ZnO (T = 300 K).

shown in the figure. However, the coverage increases steadily with dosing pressure, even at the highest pressure shown. This shows that at least part of the adsorption occurs via an activated process, and that the activation barrier becomes progressively higher as adsorption progresses.

(3) The temperature of the dominant peak, $T_m(I_b)$, shifts to lower temperature with increasing coverage (see below).

The relative magnitude of the activation barriers for adsorption into the various states is indicated more clearly by the TPD spectra shown in Fig. 4. These spectra were

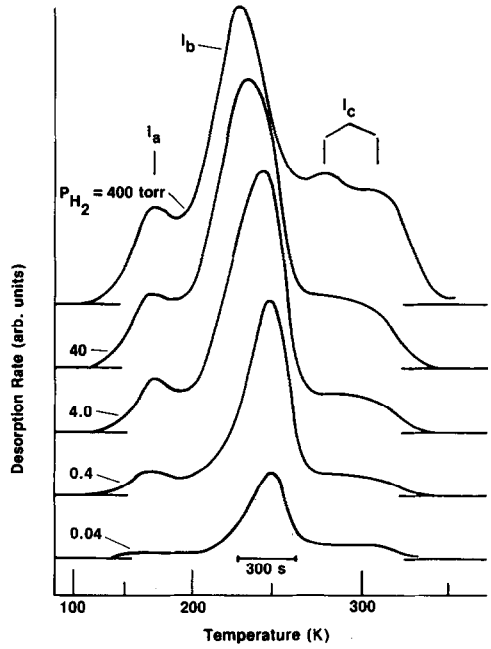

FIG. 3. Thermal TPD spectra of H_2 desorbing from ZnO. Dosage: H_2 adsorbed by cooling sample to 100 K at indicated H_2 pressure, then evacuating.

Dosing Conditions		
EXPT	P (torr)	T (K)
1)	0.4	100
2)	40.0	100
3)	40.0	300 → 100

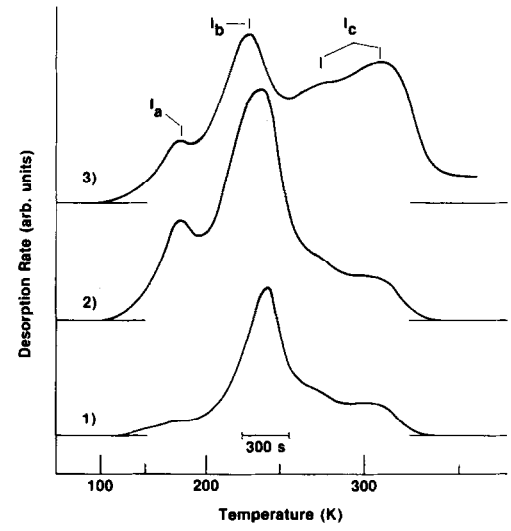

FIG. 4. H_2/ZnO thermal TPD spectra observed after various dosing procedures: (1) Exposed clean sample to 0.4 Torr H_2 at 100 K for 10 min. (2) Exposed to 40 Torr H_2 at 100 K for 10 min. (3) Exposed to 40 Torr H_2 at 300 K for 10 min, then cooled to 100 K.

made from initial coverages obtained using three different dosing procedures. Spectrum 1 was obtained by cooling the sample under vacuum to 100 K, then exposing it to 0.4 Torr of H_2 for 10 min, followed by evacuation. This procedure will populate sites with zero or a small activation barrier for adsorption ($E_a \lesssim 4$ kcal/mole). As seen from the spectrum, approximately one-half of the ultimate attainable coverage of state I_b is achieved; little adsorption into state I_a or I_c occurs.

Spectrum 2 was obtained by cooling the sample under vacuum to 100 K, exposing it to 40 Torr of H_2 for 10 min, and then evacuating. This procedure will populate sites with a moderate activation barrier for adsorption ($E_a = \sim 5$ kcal/mole). This spectrum shows that state I_b is now fully populated, and state I_a is also populated. Only a slight increase in the population of state I_c is observed.

Spectrum 3 was obtained by exposing the sample to 40 Torr of H_2 at 300 K for 10 min, then cooling to 100 K and evacuating. This will populate states with large activation barriers for adsorption ($6 \lesssim E_a \lesssim 15$ kcal/mole). State I_c is now fully populated. The peak for state I_b has also shifted to lower temperature. This suggests that the temperature shift observed here and in Fig. 3 is due to repulsive interactions between adsorbate molecules.

The ir spectra of the H_2 coverages for these three dosing procedures were recorded before beginning the warm-up and are shown in Fig. 5. The dominant features are the peaks at 3490 and 1710 cm^{-1}, which were observed in the room-temperature spectrum (cf. Fig. 2). However, a new feature appears in the OH stretching region at 3455 cm^{-1} in spectra 2 and 3. By comparing these spectra with the TPD spectra in Fig. 4, we can assign this new feature to the OH stretching mode of the I_a adsorption state. In contrast, there is no clear evidence for a similar unique feature in the ZnH stretching region due to type I_a adsorption. The type I_b and I_c adsorption states show identical ir

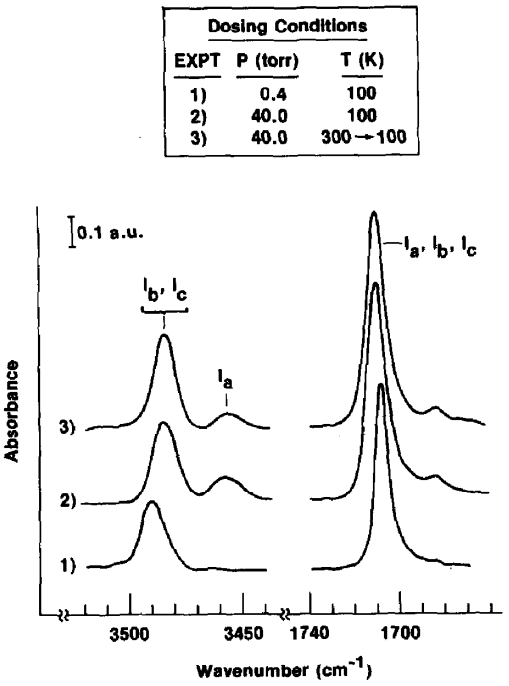

FIG. 5. Infrared spectra of H_2/ZnO as a function of dosage prior to TPD experiments (1), (2), and (3), described in Fig. 4.

behavior in both the OH and ZnH stretching regions.

Kokes *et al.* (*7*) have previously noted the existence of a discrete OH stretching feature near 3455 cm^{-1} on samples exposed to H_2 at low temperature. They also reported the analogous low-frequency feature for D_2-covered samples, thereby showing that the feature is not due to perturbation of background OH groups. As shown below, we can also demonstrate that the I_a feature is not due to a perturbation of filled I_b and I_c sites.

Further proof of the assignment of the unique ir feature at 3455 cm^{-1} to the type I_a state is given by the following experiment: A sample was cooled in 40 Torr of H_2 to 100 K and evacuated to prepare an initial H_2 coverage corresponding to the second TPD spectrum in Fig. 3, which is reproduced in Fig. 6. A series of "interrupted" TPD warm-ups were performed by heating the sample to an intermediate temperature T_i then rapidly cooling the sample to 100 K.

The ir spectrum was recorded, and another warm-up was performed, being interrupted at a higher T_i. This procedure was repeated until all of the H_2 had desorbed. The process can be viewed as a fractional depletion of the adsorbate coverage in discrete stages, with an ir spectrum recorded at each stage. The interruption temperatures are shown by the open circles on the curve in Fig. 6. The desorption spectra obtained from each warm-up, if summed on a common temperature scale, reproduce to within 10% the TPD spectrum for warm-up over the entire temperature range.

This procedure was preferred over recording ir spectra while the TPD warm-up was in progress, in order to avoid differences in the warm-up rate due to sample heating by the ir beam, and to ensure constant coverage during the recording of each ir spectrum. The ir spectra obtained at each stage of the interrupted TPD process are shown in Fig. 7. Two points are noted:

(1) After interruption at 190 K, the OH feature at 3455 cm^{-1} has disappeared, proving that it corresponds to state I_a in the TPD spectrum. In a separate experiment, state I_a was repopulated with D_2, confirming that distinct sites exist for I_a, and that the ir feature at 3455 cm^{-1} does not result from some perturbation of filled I_b or I_c sites.

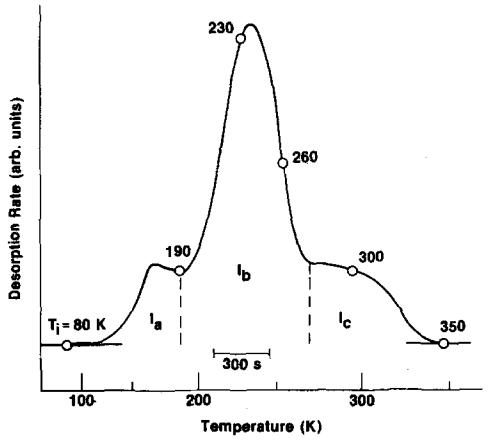

FIG. 6. Interrupted thermal TPD experiment of H_2/ZnO; full warm-up spectrum reproduced from Fig. 3. O: Interruption temperatures of successive warm-ups.

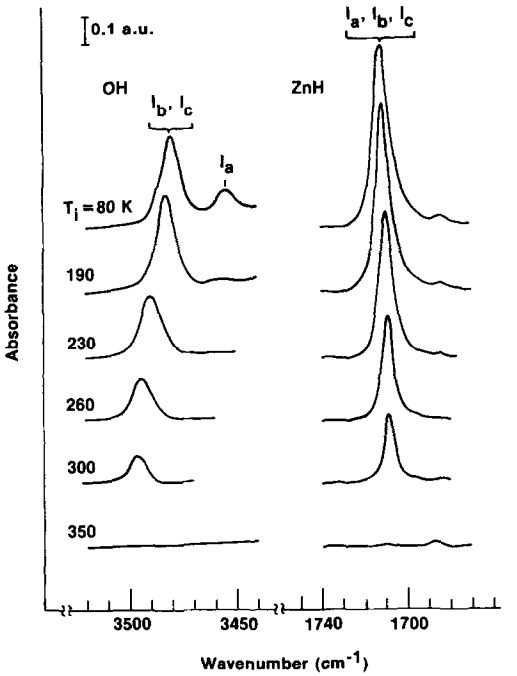

FIG. 7. Infrared spectra of H_2/ZnO recorded at 100 K after interruptions in thermal TPD warm-up shown in Fig. 6.

(2) The wavenumber shift and integrated intensity vary continuously with coverage, indicating that both type I_b and I_c states contribute to the ir features near 3490 and 1710 cm^{-1}, and that their contributions are indistinguishable on the basis of ir absorbance alone.

Further evidence of the identical ir behavior of I_b and I_c states is shown in Figs. 8 and 9. In Fig. 8 we show the integrated absorbance as a function of absolute coverage for the experiments described in Figs. 3–7. The integrated absorbance is estimated by multiplying the peak height times the FWHM. The absolute coverage is determined by integrating the area under the TPD spectrum, after calibrating the mass spectrometer and pumping system with known quantities of H_2. The solid lines represent quadratic least-square fits to the observed results; the resulting analytic expressions for the intensity vs coverage functions are used below in determining adsorption isotherms.

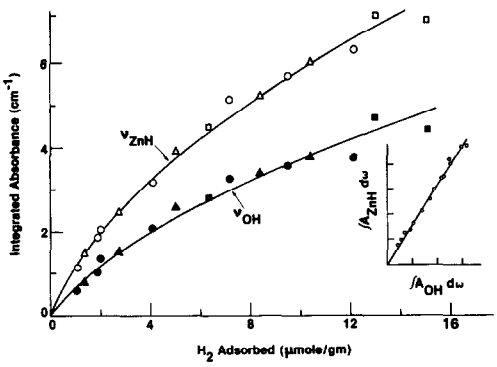

FIG. 8. Infrared intensity vs coverage for H_2/ZnO. ○, ●: Fig. 3; □, ■: Figs. 4, 5; △, ▲: Figs. 6, 7 (interrupted TPD).

The integrated intensities of both the ν_{ZnH} and ν_{OH} peaks vary continuously with coverage in a slightly nonlinear manner; the specific absorbance decreases with increasing coverage. There is no systematic variation between the experiments using coverages prepared by normal adsorption procedures, shown by circles and squares, and the experiments using the coverages obtained by interrupted TPD, shown by triangles. These two sets of coverages have different relative populations of filled I_b and I_c states. The absence of any systematic difference in the intensity vs coverage indicates that the specific absorbance of type I_b and I_c sites is the same.

The inset shows the correlation between the ν_{OH} and ν_{ZnH} absorbances for each coverage. The two peaks develop proportionally together, supporting the model of dissociative adsorption on a Zn–O pair site.

The maximum coverage observed in this work is ~15 μmole/g (= 0.34 cm^3 (STP)/g). This is somewhat greater than the highest type I coverage reported by Dent and Kokes (0.11 cm^3/g (*10*)) or by Eischens *et al.* (0.2 cm^3/g (*6*)), and may be due to differences in sample pretreatment. However, even our highest coverage corresponds to a H_2-adsorption area of only 1 m^2/g, if the surface area per adsorbed H–H pair is assumed to be 10^{-15} cm^2/H_2. This represents only 10% of the BET surface area specified by the manufacturer, and thus confirms that type I adsorption sites comprise only a fraction of the total surface area.

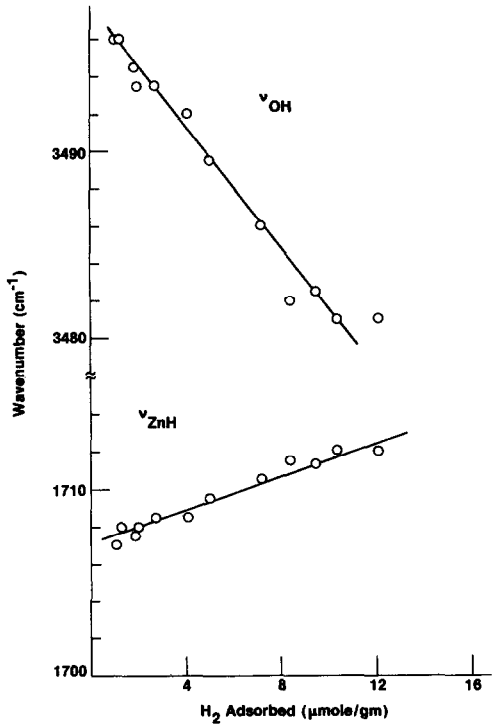

FIG. 9. Coverage dependence of ir stretching frequencies for H_2/ZnO.

Figure 9 shows the coverage dependence of the OH and ZnH stretching frequencies in the experiments shown in Figs. 3–7. The OH stretching frequency decreases by 15 cm^{-1} with increasing coverage, while the ZnH frequency increases by 5 cm^{-1}. This agrees with the shifts observed by other authors (*7, 9*). There is nothing in the frequency shift behavior to distinguish between I_b and I_c states. In particular, it is clear that frequency shift is *not* caused by the sequential filling of two states with different stretching frequencies.

Finally, in Fig. 10 we show adsorption isotherms measured at 273 and 323 K. Only states I_b and I_c are populated under these conditions, as no peak for I_a adsorption was observed at 3455 cm^{-1}. Surface coverages were determined from the integrated absorbance of the ZnH peak using the intensity vs coverage results shown in Fig. 8.

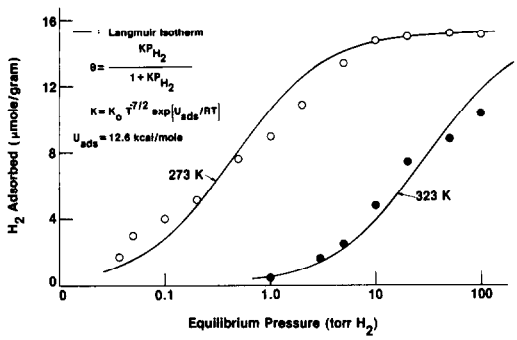

FIG. 10. Adsorption isotherms for H_2/ZnO. ○: Measured at 273 K; ●: 323 K; ——: best fit of Langmuir isotherms with uniform binding energy U_{ads} = 12.6 kcal/mole.

The sample was allowed to equilibrate for 15 min at each pressure before recording the ir spectrum. This was shown to be sufficient equilibration time, on the basis of the TPD results.

The data are very nearly described by a Langmuir isotherm with uniform binding energy, U_{ads}:

$$\theta = \frac{KP}{1 + KP}, \qquad (1)$$

$$K = K_0 T^{-7/2} \exp(U_{ads}/RT), \qquad (2)$$

where θ is the fractional coverage and K is the equilibrium constant for adsorption. The temperature dependence of the preexponential factor in Eq. (2) is derived from the statistical mechanical description of dissociative, localized adsorption (*17*).

The solid curves in Fig. 10 were calculated using Eqs. (1) and (2) and a binding energy U_{ads} = 12.6 kcal/mole. The latter was obtained by optimizing the fit of Eqs. (1) and (2) to the observed results for the two temperatures.

The observed results show a systematic deviation from the simple Langmuir isotherm, suggestive of an energetically inhomogeneous surface. The estimated magnitude of the variation in U_{ads} over the experimental coverage range is ±1 kcal/mole. As discussed further on, this is smaller than the difference between the desorption energies of states I_b and I_c obtained from analysis of the TPD spectra.

DISCUSSION

The goal of this work is to obtain quantitative information about the energetics of type I H_2 adsorption on ZnO. Kokes *et al.* (*7*) have noted that H_2 desorption is "slow" at 248 K; however, examination of their spectra recorded at 95 and 248 K reveals that some desorption has occurred at the latter temperature. In order to obtain a more detailed description of the desorption energetics, we have chosen to apply the technique of temperature-programmed desorption to this system.

The interpretation of temperature-programmed desorption spectra obtained from porous, high-surface-area materials has been discussed by Cvetanovic and Amenomiya (*18*). For the particular case of H_2 desorption from ZnO, we can make the simplifying assumption that readsorption can be neglected, because adsorption is an activated process. A quantitative comparison of the adsorption rate constant, estimated from Figs. 3 and 4, with the time scale for diffusion, estimated using a calculated Knudsen diffusion coefficient, indicates that desorbed H_2 molecules will diffuse out of the sample before they are readsorbed. Thus, the ability to neglect readsorption *for this system* will considerably simplify the interpretation of our TPD spectra.

As a result of this simplification, the familiar Redhead equation (*19*) can be used to derive values of the desorption energy, E_d, from the observed temperature maxima, T_m:

$$E_d/RT_m = \ln \frac{\nu_0 RT_m^2}{\beta E_d} \qquad (3)$$

Here β is the heating rate during the warm-up and ν_0 is the preexponential factor for the desorption process. Equation (3) is based on first-order desorption kinetics, which is a reasonable assumption for the case of H_2 molecules desorbing from local-

TABLE 1

Desorption Energies and ir Stretching Frequencies of Type I_a, I_b, and I_c Binding Sites for H_2/ZnO

TPD state	T_m (K)	E_d[a] (kcal/mole)	ν_{OH}[b] (cm^{-1})	ν_{ZnH}[b] (cm^{-1})
I_a	173	12	3455	1707
I_b	232	16	3498	1707
I_c	(279)	(19)	3498	1707
	305	21	3498	1707

[a] Assumed first-order desorption kinetics, $\nu_0 = 10^{13}$ s^{-1}.

[b] Extrapolated to zero coverge.

ized Zn–O pair sites. In using Eq. (3), we assume the conventional value of $\nu_0 = 10^{13}$ s^{-1} for the preexponential factor.

In Table 1 we list the observed temperature maxima and the corresponding desorption energies for the TPD spectrum of the highest coverage shown in Fig. 3, along with the ir stretching frequencies of each state, extrapolated to zero coverage. We note that there is a 5 kcal/mole difference between the kinetically estimated desorption energies of states I_b and I_c. This is in contrast with the isotherm measurements described before, which indicated a maximum variation of ~2 kcal/mole in the binding energy, U_{ads}, of states I_b and I_c. The difference in kinetic desorption energies is also in contrast with the fact that the two states show identical ir behavior. Thus, the two states are distinguished by different activation barriers, which do not affect the shape of the potential energy surface for each state near the potential minimum, and hence do not affect the ir stretching frequencies.

It was noted above that the temperature maximum for the type I_b state decreased with coverage. In Table 2 we list the observed values of T_m and the calculated values of E_d for the I_b states for each of the initial coverages shown in Fig. 3. The desorption activation energies are seen to decrease with increasing coverage, which may be a result either of site heterogeneity within the ensemble of type I_b sites, or of repulsive interactions between adsorbed species. We favor the latter explanation, in view of the fact that filling the I_c sites also shifts the I_b peak to lower temperature (cf. Fig. 4). This also suggests that the I_b and I_c sites are in close proximity. The magnitude of the observed decrease in desorption activation energy, 1.2 kcal/mole, is the order expected for static dipole–dipole repulsion between two OH groups separated by 3.25 Å, the O^{2-} anion separation distance in ZnO.

By combining the desorption energies determined from the TPD spectra, the binding energies determined from the adsorption isotherms, and the activation barriers estimated from the adsorption kinetics, we can construct schematic Polanyi diagrams for each of the binding states observed in this work. These are shown in Fig. 11.

The most weakly bound state, I_a, has an activation barrier of about 5 kcal/mole, and a desorption energy of 12 kcal/mole. The binding energy inferred from these is 7 kcal/mole, which is consistent with the fact that this state cannot be populated at room temperature and the H_2 pressures studied here. This state has a distinct OH stretching frequency of 3455 cm^{-1} further distinguishing it from states I_b and I_c.

The I_b state has an activation barrier of $\gtrsim$4 kcal/mole, a binding energy of ~12 kcal/mole, and a desorption energy of ~16

TABLE 2

Coverage Dependence of H_2 Desorption Energy from Type I_b Binding Sites

H_2 coverage[a] (μmole/g)	T_m (K)	E_d[b] (kcal/mole)
1.8	249.1	16.9
3.8	249.3	16.9
6.5	243.8	16.5
8.5	236.8	16.0
10.8	232.2	15.7

[a] Total coverage in type I_b and I_c sites.

[b] Assuming first-order desorption kinetics, $\nu_0 = 10^{13}$ s^{-1}.

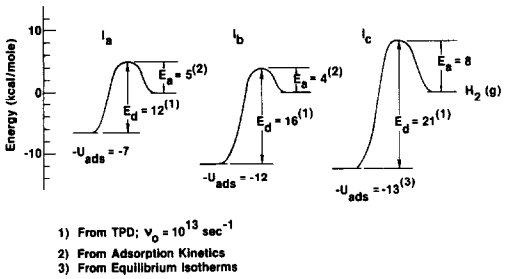

FIG. 11. Energetics of type I adsorption states for H_2 on ZnO.

kcal/mole. As noted above, the activation barrier for adsorption may increase slightly with increasing coverage (~1 kcal/mole). Combined with the coverage-dependent decrease in desorption activation energy shown in Table 2, this implies that the binding energy decreases by a total of ~2 kcal/mole with increasing coverage. This is within the range of site heterogeneity indicated by the isotherm data.

The highest I_c state has a desorption energy of 21 kcal/mole. If we assign the largest binding energy consistent with the isotherm data, namely, 13 kcal/mole, then the activation barrier is ~8 kcal/mole. Such a large value is consistent with the difficulty of filling type I_c sites indicated in Fig. 4.

We can conclude from Fig. 11 that the I_a adsorption state has a unique potential energy surface, when compared to the I_b and I_c adsorption states. In contrast, the potential energy surfaces of the I_b and I_c states are quite similar to each other, and differ only with respect to the magnitude of their activation barriers. Apparently, the factors which produce the different activation barriers for these two states do not change the potential energy surfaces in the neighborhood of the equilibrium adsorbate configuration, as indicated by the observed similarity in vibrational frequencies and binding energies.

SUMMARY

Results from ir and TPD experiments have been combined to obtain a detailed picture of the energetics of type I H_2 adsorption on ZnO. The TPD experiments resolve three distinct binding states, which we have labeled types I_a, I_b, and I_c, in order of increasing desorption activation energy. The I_a state has a unique OH stretching frequency at 3455 cm^{-1} and a much lower binding energy than the I_b and I_c states, so that it can be populated only at low temperatures. The I_b and I_c states have indistinguishable ir spectra and essentially equal binding energies, and can be populated at room temperature and H_2 pressures >1 Torr. The I_b and I_c states are distinguished by different activation barriers for adsorption, with state I_c having the larger barrier.

REFERENCES

1. Denny, P. J., and Whan, D. A., *in* "Catalysis" (D. A. Dowden and C. Kemball, Eds.), Vol. 2, p. 46. Specialist Periodic Reports, The Chemical Society, London, 1977.
2. Kokes, R. J., and Dent, A. L., *in* "Advances in Catalysis and Related Subjects," Vol. 22, p. 1. Academic Press, New York, 1972.
3. Cunningham, J., Finn, E., and Samman, N., *Discuss. Faraday Soc.* **58,** 160 (1974).
4. Bard, A. J., *Science* **207,** 139 (1980).
5. Herman, R. G., Klier, K., Simmons, G. W., Finn, B. P., Bulko, J. B., and Kobylinski, T. P., *J. Catal.* **56,** 407 (1979).
6. Eischens, R. P., Pliskin, W. A., and Low, M. J. D., *J. Catal.* **1,** 180 (1962).
7. Kokes, R. J., Dent, A. L., Chang, C. C., and Dixon, L. T., *J. Amer. Chem. Soc.* **94,** 4429 (1972).
8. Naito, S., Shimizu, H., Hagiwara, E., Onishi, T., and Tamaru, K., *Trans. Faraday Soc.* **67,** 1519 (1971).
9. Boccuzzi, F., Borello, E., Zecchina, A., Bossi, A., and Camia, M., *J. Catal.* **51,** 150 (1978).
10. Dent, A. L., and Kokes, R. J., *J. Phys. Chem.* **73,** 3773 (1969).
11. Baranski, A., and Galuszka, J., *J. Catal.* **44,** 259 (1976).
12. Baranski, A., and Cvetanovic, R. J., *J. Phys. Chem.* **75,** 208 (1971).
13. Chang, C. C., Dixon, L. T., and Kokes, R. J., *J. Phys. Chem.* **77,** 2634 (1973).
14. Taylor, J. H., and Amberg, C. H., *Canad. J. Chem.* **39,** 535 (1961).
15. Amberg, C. H., and Seanor, D. A., *in* "Proceedings, 3rd International Congress on Catalysis, Amsterdam, 1964" (W. M. H. Sachtler *et al.*, Eds.), paper I.22. North-Holland, Amsterdam, 1964.

16. Little, L. H., "Infrared Spectra of Adsorbed Species, p. 79 ff. Academic Press, New York, 1966.
17. Clark, A., "The Theory of Adsorption and Catalysis," p. 21 ff. Academic Press, New York, 1970.
18. Cvetanovic, R. J., and Amenomiya, Y., *in* "Advances in Catalysis and Related Subjects," Vol. 17, p. 103. Academic Press, New York, 1967.
19. Redhead, P. A., *Vacuum* **12,** 203 (1962).